


RESEARCH

Open Access



# Association of A $\beta$ deposition and regional synaptic density in early Alzheimer's disease: a PET imaging study with [ $^{11}\text{C}$ ]UCB-J

Ryan S. O'Dell<sup>1,2</sup>, Adam P. Mecca<sup>1,2</sup>, Ming-Kai Chen<sup>3</sup>, Mika Naganawa<sup>3</sup>, Takuya Toyonaga<sup>3</sup>, Yihuan Lu<sup>3</sup>, Tyler A. Godek<sup>1,2</sup>, Joanna E. Harris<sup>1,2</sup>, Hugh H. Bartlett<sup>1,2</sup>, Emmie R. Banks<sup>1,2</sup>, Victoria L. Kominek<sup>1,2</sup>, Wenzhen Zhao<sup>1,2</sup>, Nabeel B. Nabulsi<sup>3</sup>, Jim Ropchan<sup>3</sup>, Yunpeng Ye<sup>3</sup>, Brent C. Vander Wyk<sup>4</sup>, Yiyun Huang<sup>3</sup>, Amy F. T. Arnten<sup>5</sup>, Richard E. Carson<sup>3</sup> and Christopher H. van Dyck<sup>1,2,5,6\*</sup> 

## Abstract

**Background:** Attempts to associate amyloid- $\beta$  (A $\beta$ ) pathogenesis with synaptic loss in Alzheimer's disease (AD) have thus far been limited to small numbers of postmortem studies. A $\beta$  plaque burden is not well-correlated with indices of clinical severity or neurodegeneration—at least in the dementia stage—as deposition of A $\beta$  reaches a ceiling. In this study, we examined in vivo the association between fibrillar A $\beta$  deposition and synaptic density in early AD using positron emission tomography (PET). We hypothesized that global A $\beta$  deposition would be more strongly inversely associated with hippocampal synaptic density in participants with amnesic mild cognitive impairment (aMCI; a stage of continued A $\beta$  accumulation) compared to those with dementia (a stage of relative A $\beta$  plateau).

**Methods:** We measured SV2A binding ([ $^{11}\text{C}$ ]UCB-J) and A $\beta$  deposition ([ $^{11}\text{C}$ ]PiB) in 14 participants with aMCI due to AD and 24 participants with mild AD dementia. Distribution volume ratios (DVR) with a cerebellar reference region were calculated for both tracers to investigate the association between global A $\beta$  deposition and SV2A binding in hippocampus. Exploratory analyses examined correlations between both global and regional A $\beta$  deposition and SV2A binding across a broad range of brain regions using both ROI- and surface-based approaches.

(Continued on next page)

\* Correspondence: [christopher.vandyck@yale.edu](mailto:christopher.vandyck@yale.edu)

<sup>1</sup>Alzheimer's Disease Research Unit, Yale University School of Medicine, One Church Street, 8th Floor, New Haven, CT 06510, USA

<sup>2</sup>Department of Psychiatry, Yale University School of Medicine, 300 George Street, New Haven, CT 06510, USA

Full list of author information is available at the end of the article



© The Author(s). 2021 **Open Access** This article is licensed under a Creative Commons Attribution 4.0 International License, which permits use, sharing, adaptation, distribution and reproduction in any medium or format, as long as you give appropriate credit to the original author(s) and the source, provide a link to the Creative Commons licence, and indicate if changes were made. The images or other third party material in this article are included in the article's Creative Commons licence, unless indicated otherwise in a credit line to the material. If material is not included in the article's Creative Commons licence and your intended use is not permitted by statutory regulation or exceeds the permitted use, you will need to obtain permission directly from the copyright holder. To view a copy of this licence, visit <http://creativecommons.org/licenses/by/4.0/>. The Creative Commons Public Domain Dedication waiver (<http://creativecommons.org/publicdomain/zero/1.0/>) applies to the data made available in this article, unless otherwise stated in a credit line to the data.

(Continued from previous page)

**Results:** We observed a significant inverse association between global A $\beta$  deposition and hippocampal SV2A binding in participants with aMCI ( $r = -0.55$ ,  $P = 0.04$ ), but not mild dementia ( $r = 0.05$ ,  $P = 0.82$ ; difference statistically significant by Fisher  $z = -1.80$ ,  $P = 0.04$ ). Exploratory analyses across other ROIs and whole brain analyses demonstrated no broad or consistent associations between global A $\beta$  deposition and regional SV2A binding in either diagnostic group. ROI-based analyses of the association between regional A $\beta$  deposition and SV2A binding also revealed no consistent pattern but suggested a “paradoxical” positive association between local A $\beta$  deposition and SV2A binding in the hippocampus.

**Conclusions:** Our findings lend support to a model in which fibrillar A $\beta$  is still accumulating in the early stages of clinical disease but approaching a relative plateau, a point at which A $\beta$  may uncouple from neurodegenerative processes including synaptic loss. Future research should investigate the relationship between A $\beta$  deposition and synaptic loss in larger cohorts beginning preclinically and followed longitudinally in conjunction with other biomarkers.

**Keywords:** SV2A, Synaptic density, A $\beta$ , Alzheimer's disease, [ $^{11}\text{C}$ ]UCB-J PET, [ $^{11}\text{C}$ ] PiB PET

## Introduction

The concept that Alzheimer's disease (AD) is initiated by the progressive accumulation of the amyloid- $\beta$  peptide (A $\beta$ ) in brain regions important for cognition is currently the leading theory of causation but remains controversial [1]. A loss of synapses has long been recognized as perhaps the strongest neuropathological correlate of cognitive impairment in AD [1–3]. A refinement of the amyloid hypothesis is thus based on convergent evidence that A $\beta$  oligomers, the most neurotoxic A $\beta$  species, impair both synaptic function (e.g., long-term potentiation) and synaptic structure (e.g., dendritic spines) [4, 5]. A $\beta$  plaques, themselves comprised of fibrillar A $\beta$ , are thought to have a penumbra of soluble A $\beta$  oligomers in which synaptic density is low, whereas synapse number normalizes at greater distances from the plaque core [6]. Attempts to associate A $\beta$  pathogenesis with synaptic loss have thus far been limited to a small number of postmortem [7, 8] and transgenic mouse [6, 9–11] studies.

The ability to assess synaptic density *in vivo* would be of great utility for tracking AD progression and monitoring the efficacy of potential therapies. A novel molecular target is synaptic vesicle glycoprotein 2 (SV2), an essential presynaptic vesicle membrane protein whose isoform SV2A is ubiquitously expressed in virtually all synapses [12, 13]. To assess the spatiotemporal distribution of synaptic density *in vivo*, a PET tracer for SV2A known as [ $^{11}\text{C}$ ]UCB-J has previously been developed and advanced for human studies [14–16]. The specific utility of SV2A imaging as a synaptic marker relevant to AD was exemplified by our initial study using this novel SV2A PET tracer, in which we reported significant reductions in SV2A hippocampal binding in patients with amnesic mild cognitive impairment (aMCI) and mild AD dementia [17]. In our subsequent study of [ $^{11}\text{C}$ ]UCB-J in early AD in a larger cohort, we observed more extensive cortical and subcortical reductions in SV2A binding, most

pronounced in the hippocampus and entorhinal cortex and more widespread than reductions in gray matter volume [18]. When the AD group was separated into aMCI and dementia subgroups, these patterns were observed at both stages of disease [18]. These results are consistent with the subset of postmortem studies that have examined the prodromal or mild stages of AD [19–24]. These studies have focused primarily on hippocampus as the site of the earliest and most profound synaptic loss [19–21], consistent with the early degeneration of entorhinal cortical cells projecting via the perforant path to the hippocampus [25, 26].

As a general principle, A $\beta$  plaque burden is not well-correlated with indices of symptom duration and severity—at least in the dementia stage—as deposition of A $\beta$  reaches a ceiling [27–29]—suggesting a dynamic balance between A $\beta$  deposition and clearance [28, 29]. In the era of A $\beta$  PET imaging, this ceiling has been better defined longitudinally, and brain A $\beta$  load has been shown to approach a “plateau” [30]. Longitudinal studies have generally demonstrated continued A $\beta$  accumulation through the prodromal stages of AD [31–33], with minimal change by the time of conversion to AD dementia [31, 34] or in the dementia stage [35]. Therefore, in the prodromal stage of AD, when A $\beta$  plaques are still accumulating, we might expect them to be associated with indices of severity, including synaptic loss—particularly in those brain regions that show marked early synaptic loss, such as hippocampus.

In this study, we examined the association between fibrillar A $\beta$  deposition with [ $^{11}\text{C}$ ] PiB PET and synaptic density with [ $^{11}\text{C}$ ]UCB-J in early AD. We hypothesized that global A $\beta$  deposition would be more strongly inversely associated with hippocampal synaptic density in the aMCI stage than the mild dementia stage. Given some *in vitro* evidence for local associations between A $\beta$  plaques and synaptic abnormalities [6, 8, 10, 11], we also

conducted exploratory correlational analyses of both global and regional A $\beta$  deposition with synaptic density in a broad range of cortical and subcortical regions.

## Methods

Detailed methods and statistical analyses are further described in the Supplementary Methods (Additional file 1).

### Study participants and design

Individuals aged 55–85 years were screened to ensure diagnostic eligibility. Participants with dementia met diagnostic criteria for probable dementia due to AD [36], had a Clinical Dementia Rating (CDR) score of 0.5–1.0 points, and a Mini-Mental Status Examination (MMSE) score  $\leq$  26 points. Participants with MCI met diagnostic criteria for amnesic MCI [37], had a CDR score of 0.5 points, and a MMSE score of 24–30 points. All participants with dementia and aMCI demonstrated impaired episodic memory, as evidenced by a Logical Memory II (LMII) score 1.5 standard deviations below an education-adjusted norm. Cognitively normal (CN) participants had a CDR score of 0, an MMSE score  $>$  26, and a normal education-adjusted LMII score. The Rey Auditory Verbal Learning Test (RAVLT) was also administered to generate an episodic memory score, calculated by averaging the RAVLT and LMII  $z$ -scores. *APOE* genotyping was performed as in our previous study [38]. Participants with dementia and aMCI were required to be A $\beta$ <sup>+</sup> and all CN participants A $\beta$ <sup>-</sup>, according to their [<sup>11</sup>C] PiB scans (Additional file 1). All participants provided written informed consent as approved by the Yale University Human Investigation Committee prior to participating in the study.

### Brain imaging

T1-weighted magnetic resonance imaging (MRI) was performed to define regions of interest (ROI) and to perform partial volume correction (PVC) using the Iterative Yang (IY) algorithm [39, 40]. PET scans were performed on the HRRT (207 slices, resolution  $<$  3 mm full width half max [FWHM]), the highest resolution human PET scanner [41]. List-mode data were reconstructed using the MOLAR algorithm [42] with event-by-event motion correction based on an optical detector (Vicra, NDI Systems, Waterloo, Canada) [43]. Dynamic [<sup>11</sup>C] PiB scans were acquired for 90 min following administration of a bolus of up to 555 MBq of tracer [38], while dynamic [<sup>11</sup>C]UCB-J scans were acquired for 60 min after administration of a bolus of up to 740 MBq [16]. Software motion correction was applied to the dynamic PET images using a mutual-information algorithm (FSL-FLIRT) to perform frame-by-frame registration to a summed image (0–10 min). A summed motion-corrected PET image was registered to each participant's MRI. Cortical

reconstruction and volumetric segmentation was performed using FreeSurfer [version 6.0] [44]. Specific ROIs utilized for [<sup>11</sup>C] PiB and [<sup>11</sup>C]UCB-J analyses in this study included medial temporal (entorhinal, hippocampus, parahippocampal, amygdala), prefrontal, lateral temporal, posterior cingulate/precuneus, anterior cingulate, lateral parietal, lateral occipital, medial occipital, and pericentral ROIs, as previously described (Supplementary Tables 1 & 2 from [18]). Global A $\beta$  deposition was determined for a composite of regions commonly affected by A $\beta$  deposition in AD which included prefrontal, lateral temporal, posterior cingulate/precuneus, and lateral parietal ROIs.

**Tracer kinetic modeling** For [<sup>11</sup>C] PiB image analysis, parametric images of  $BP_{ND}$  were generated using a simplified reference tissue model—2 step (SRTM2) from 0 to 90 min [45] with whole cerebellum as the reference region as previously described [18, 38]. These values were then directly converted to distribution volume ratios ( $DVR$ ), in that  $DVR = BP_{ND} + 1$ . For [<sup>11</sup>C]UCB-J image analysis, parametric images of  $BP_{ND}$  were generated using a SRTM2 from 0 to 60 min [45] and a small ROI (2 mL) in the core of the centrum semiovale (CS) as the reference region [46]. SRTM2 requires a global clearance rate constant of the reference region ( $k'_2$ ), which was previously computed as a population average of  $k_2$  of the CS obtained using the 1TC model ( $k'_2 = 0.027 \text{ min}^{-1}$ ) [18]. As previously described, values of  $DVR$  using a whole cerebellum reference region were then computed for each voxel as  $(BP_{ND} + 1)/(BP_{ND} [\text{cerebellum}] + 1)$  [18], which was used as the primary outcome measure for [<sup>11</sup>C]UCB-J. In a separate sample, conversion of  $BP_{ND}$  with a CS reference region to values of  $DVR$  with a cerebellar reference region was validated by comparison against regional values of [<sup>11</sup>C]UCB-J  $DVR$  calculated directly with a cerebellar reference region using the SRTM2 model from 0 to 60 min and  $DVR$  calculated from the 1-tissue compartment (1TC) model using metabolite-corrected arterial plasma curves and a cerebellar reference region (Additional file 1, Supplementary Figure 1). For whole-cortex surface-based correlations between synaptic density and A $\beta$  deposition, parametric PET images were co-registered to native subject space, sampled onto the cortical surface, and spatially smoothed with a 10 mm FWHM Gaussian kernel prior to statistical analysis.

### Statistical analyses

Statistical analyses are described in detail in the Supplementary Methods (Additional file 1). Briefly, characteristics of the participant groups were compared using  $\chi^2$  test for categorical variables and unpaired  $t$ -tests for continuous variables.

Separate linear mixed models were used to compare [ $^{11}\text{C}$ ] PiB DVR and [ $^{11}\text{C}$ ]UCB-J DVR across multiple ROIs between CN, aMCI, and dementia groups, with post hoc tests including ANOVAs within each ROI followed by unpaired  $t$ -tests for between-group comparisons within an ROI. The Benjamini-Hochberg procedure was used to control the false discovery rate (FDR) for multiple comparisons (12 comparisons for ROIs, and 3 comparisons for diagnostic groups). For the primary analysis of the association between global A $\beta$  deposition and hippocampal synaptic density in participants with aMCI and dementia, separate univariate regression analyses were performed for each diagnostic group with correlation coefficients (Pearson  $r$ ) and associated two-tailed  $P$  values reported for each model. For sensitivity analyses, separate multiple linear regression models were fit that also included covariates of age and sex. Based on our primary hypothesis of stronger correlation in aMCI than dementia, Fisher  $z$ -transformation was used to assess for significant differences in correlation coefficients between the aMCI and dementia groups, with one-tailed  $P$  values reported. Exploratory analyses assessed the relationships between global A $\beta$  deposition and regional synaptic density, as well as intra-regional A $\beta$  deposition and synaptic density (both regional- and surface-based approaches) using Pearson  $r$  correlation and associated two-tailed  $P$  values. Correction for multiple comparisons was not performed for exploratory analyses.

The contribution of partial volume effects on all aforementioned analyses was evaluated through application of PVC (Additional file 1).

## Results

### Participant characteristics

The study sample consisted of 57 participants—14 with aMCI due to AD, 24 with mild AD dementia, and 19 who were CN. This sample substantially overlapped that in our previous study [18] but included 4 additional participants with mild AD dementia. Diagnostic groups were well balanced for age ( $F(2,54) = 0.30, P = 0.74$ ) and sex ( $\chi^2 = 2.55, P = 0.28$ ), with the CN group demonstrating significantly more years of education than the dementia group (Table 1; CN: 17.7 years  $\pm$  2.1, dementia: 15.8 years  $\pm$  2.4, unpaired  $t$ -test,  $P = 0.02$ ). The symptomatic groups had clinical characteristics typical of aMCI and mild dementia with significant deficits in cognition (MMSE; aMCI: 26.3  $\pm$  2.9, dementia: 21.5  $\pm$  3.0) and function (CDR sum of boxes; aMCI: 2.3  $\pm$  1.0, dementia: 5.3  $\pm$  1.5) in comparison to the CN participants (MMSE = 29.2  $\pm$  1.1, CDR sum of boxes = 0.0  $\pm$  0.0). Regarding *APOE* genotype, typical of such samples, 21.1% of CN, 64.3% of aMCI, and 70.8% dementia participants carried at least one copy of *APOE*  $\epsilon 4$ .

**Table 1** Participant demographics and test results

	Cognitively normal	Mild cognitive impairment	Mild dementia	$F/\chi^2$	$P$
Participants ( $n$ )	19	14	24		
Sex (M/F)	9/10	9/5	9/15	2.55	0.28
Age (years)	71.5 (7.6)	71.6 (4.2)	69.9 (9.2)	0.30	0.74
Education (years)	17.7 (2.1)	17.3 (1.9)	15.8 (2.4)*	4.71	0.013
CDR-global	0 (0)	0.5 (0)***	0.88 (0.22)***,†††	194.90	< 0.0001
CDR-SB	0 (0)	2.32 (1.03)***	5.25 (1.52)***,†††	119.72	< 0.0001
GDS	0.68 (0.82)	2.79 (2.15)*	1.50 (1.84)	6.40	0.003
UPSIT	34.05 (5.86)	22.64 (9.79)**	21.09 (6.95)***	17.35	< 0.0001
MMSE	29.21 (1.13)	26.29 (2.89)*	21.46 (2.98)***,†††	52.88	< 0.0001
LMII	13.58 (4.38)	3.57 (2.98)***	0.25 (0.44)***,†	113.55	< 0.0001
RAVLT-delay	11.05 (2.80)	2.14 (2.71)***	0.29 (0.69)***,†	143.61	< 0.0001
Episodic memory (z-score)	1.25 (0.52)	-0.35 (0.39)***	-0.78 (0.08)***,†	177.54	< 0.0001
<i>APOE</i> $\epsilon 4$ copy number ( $n$ )				14.95	0.005
2 copies	0 (0%)	5 (35.7%)	5 (20.8%)		
1 copy	4 (21.1%)	4 (28.6%)	12 (50.0%)		
0 copies	15 (78.9%)	5 (35.7%)	7 (29.2%)		

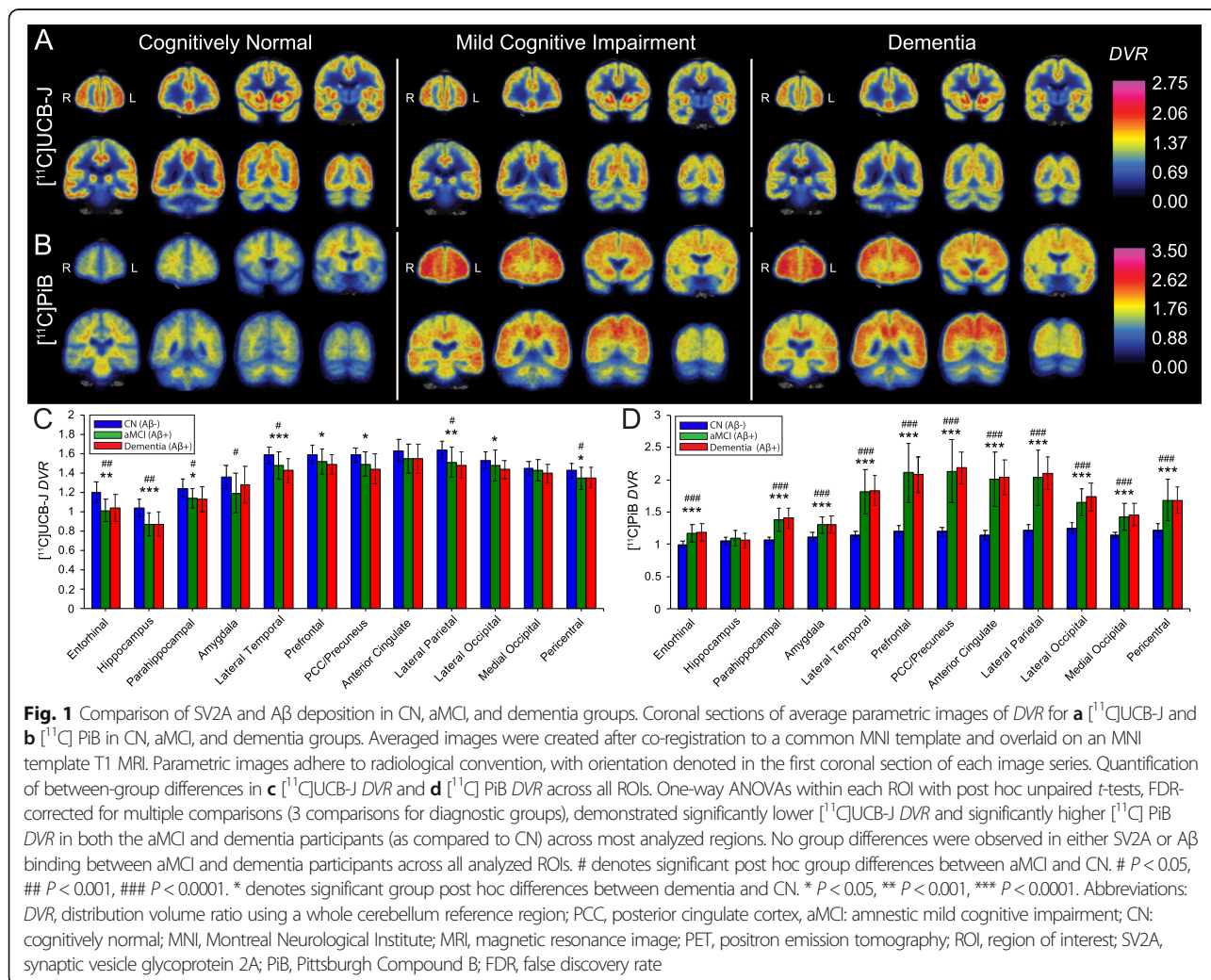
Data for continuous variables are mean (SD). Data for *APOE* copy number are  $n$  (percent).  $F$  statistics and  $P$  values are from one-way ANOVA significance tests.  $\chi^2$  statistics and  $P$  values for counts are from  $\chi^2$  significance tests. Post hoc unpaired  $t$ -tests after one-way ANOVA for continuous variables were Bonferroni corrected for 3 diagnostic groups. \* denotes significant group differences between either amnesic mild cognitive impairment and cognitively normal or mild dementia and cognitively normal. \*  $P < 0.05$ , \*\*  $P < 0.001$ , \*\*\*  $P < 0.0001$ . † denotes significant group differences between mild dementia and amnesic mild cognitive impairment. †  $P < 0.05$ , ††  $P < 0.001$ , †††  $P < 0.0001$ . Episodic Memory was calculated by averaging the z-scores of the RAVLT and LMII. *Abbreviations:* CDR-global clinical dementia rating global score, CDR-SB clinical dementia rating sub of boxes, MMSE Mini-Mental State Examination, LMII Logical Memory II score, RAVLT Rey Auditory Verbal Learning Test, GDS Geriatric Depression Scale, UPSIT University of Pennsylvania Smell Identification Test, *APOE* Apolipoprotein E

### Distribution of synaptic density and A $\beta$ deposition in normal cognition, aMCI, and dementia

Analyses of both [ $^{11}\text{C}$ ]UCB-J and [ $^{11}\text{C}$ ] PiB *DVR* demonstrated significant effects of group ([ $^{11}\text{C}$ ]UCB-J:  $F(2,54) = 10.1$ ,  $P = 0.0002$ , [ $^{11}\text{C}$ ]PiB:  $F(2,54) = 56.9$ ,  $P < 0.0001$ ), ROI ([ $^{11}\text{C}$ ]UCB-J:  $F(11,594) = 318.9$ ,  $P < 0.0001$ , [ $^{11}\text{C}$ ]PiB:  $F(11,594) = 257.4$ ,  $P < 0.0001$ ), and group  $\times$  ROI interaction ([ $^{11}\text{C}$ ]UCB-J:  $F(22,594) = 2.3$ ,  $P = 0.001$ , [ $^{11}\text{C}$ ]PiB:  $F(22,594) = 43.3$ ,  $P < 0.0001$ ) as predictors of SV2A and A $\beta$  binding. Consistent with our recent publication [18], one-way ANOVA with post hoc, false discovery rate (FDR)-corrected unpaired *t*-tests revealed significant reductions of SV2A binding in both aMCI and dementia participants (compared to CN) across the majority of neocortical regions, with the exception of the anterior cingulate and medial occipital cortices (Fig. 1a, c, Supplementary Table 1). Group differences were largest in the hippocampus, entorhinal cortex, and lateral temporal cortex. The prefrontal, PCC/precuneus, and lateral occipital cortices also demonstrated significant reductions in SV2A binding

in the dementia group, while non-significant trends of SV2A reduction were observed in aMCI participants (as compared to the CN group). One-way ANOVA with post hoc, FDR-corrected unpaired *t*-tests of [ $^{11}\text{C}$ ] PiB revealed significant and broadly distributed A $\beta$  deposition across all neocortical regions in both aMCI and dementia (compared to CN) participants, with the exception of the hippocampus (Fig. 1b, d, Supplementary Table 2). No differences were observed in either SV2A or A $\beta$  binding between aMCI and dementia groups across all analyzed ROIs. Average group images of *DVR* demonstrated visible reduction and deposition of SV2A and A $\beta$  binding, respectively, in both aMCI and dementia groups (Fig. 1a, b), compared to the CN group.

Volumetric MRI was used to investigate gray matter volume differences between CN, MCI, and dementia groups (Supplementary Table 3). Correction for partial volume effects revealed continued significant reductions of SV2A binding in medial temporal regions in both participants with aMCI and dementia, as well as lateral



parietotemporal reductions of SV2A binding in the dementia group only. After correction for partial volume effects, A $\beta$  deposition remained significantly elevated across all neocortical regions in both aMCI and dementia participants, with the exception of the hippocampus (Supplementary Figure 2, Supplementary Tables 1 & 2).

#### Association of global A $\beta$ deposition and regional synaptic density in aMCI and dementia

The primary analysis investigated the association of global A $\beta$  deposition and hippocampal synaptic density (SV2A binding; Fig. 2). We hypothesized that in participants with aMCI (a stage of continued A $\beta$  accumulation) but not in those with dementia (a stage of relative A $\beta$  plateau), global A $\beta$  deposition would be inversely associated with synaptic density in the hippocampus. Separate univariate linear regressions for aMCI and dementia groups demonstrated a significant inverse association in participants with aMCI ( $r = -0.55$ ,  $P = 0.04$ ) but not in those with dementia ( $r = 0.05$ ,  $P = 0.82$ ). This difference between group correlation coefficients was significant (Fisher  $z = -1.80$ , one-tailed  $P = 0.04$ ). Addition of age and sex as covariates to this model reduced the previously observed significance in the aMCI group ( $R^2 = 0.36$ , semi-partial correlation coefficient =  $-0.48$ ,  $P = 0.09$ ), while the association between global A $\beta$  deposition and hippocampal SV2A in the dementia group remained non-significant ( $R^2 = 0.24$ , semi-partial

correlation coefficient =  $0.07$ ,  $P = 0.72$ ). When participants from the aMCI and dementia groups were pooled ( $n = 38$ ), the inverse association between global A $\beta$  and hippocampal SV2A was not significant (Pearson  $r = -0.24$ ,  $P = 0.58$ ). Secondary exploratory analyses across multiple ROIs suggested no broad associations between global A $\beta$  deposition and regional SV2A in either diagnostic group (Table 2). However, a nominal inverse association was observed between global A $\beta$  deposition and lateral parietal SV2A in the dementia group ( $r = -0.43$ ,  $P = 0.03$ ).

Exploratory whole brain analyses were also performed on both a regional and surface-based level. On a regional level, the relationship between global A $\beta$  deposition and SV2A binding in all FreeSurfer regions suggested negative correlations with right-sided subcortical structures in aMCI participants, including the hippocampus, amygdala, caudate, accumbens area, and ventral diencephalon (Fig. 3a). In participants with dementia, however, inverse associations were observed primarily with right-sided cortical regions, including caudal middle frontal, pars triangularis, supramarginal, superior parietal, and inferior parietal regions (Fig. 3b). Surface-based analyses of these same relationships revealed that global A $\beta$  was negatively correlated with SV2A binding in a small cluster of vertices within the right lateral temporal cortex in participants with aMCI (Supplementary Figure 3A). In participants with dementia, by contrast, negative

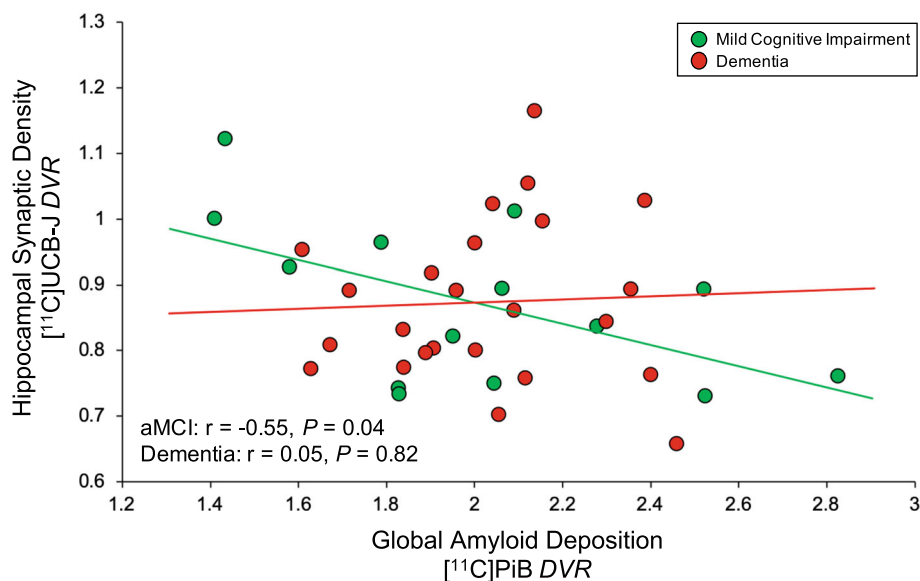


**Fig. 2** Correlation of global A $\beta$  deposition and hippocampal SV2A in aMCI and dementia due to AD. Scatter plot with best-fit lines depicts a significant inverse association between global A $\beta$  deposition and hippocampal SV2A in participants with aMCI (green) but not with dementia (red). Correlation coefficients were calculated from separate univariate linear regression analyses in each group with associated two-tailed  $P$  values, without correction for multiple comparisons. Global A $\beta$  deposition was calculated by averaging values of [11C] PiB DVR from the bilateral prefrontal, lateral temporal, posterior cingulate/precuneus, and lateral parietal ROIs, weighted by volume. Green circles denote DVR values for aMCI participants, while red circles denote DVR values for participants with dementia. Abbreviations: DVR, distribution volume ratio using a whole cerebellum reference region; aMCI: amnesic mild cognitive impairment; SV2A, synaptic vesicle glycoprotein 2A; PiB, Pittsburgh Compound B

**Table 2** Correlation of global A $\beta$  deposition and regional SV2A in aMCI and dementia due to AD

Primary region	Mild cognitive impairment (n = 14)		Dementia (n = 24)		Fisher z-transform	
	Pearson <i>r</i>	<i>P</i>	Pearson <i>r</i>	<i>P</i>	<i>z</i>	<i>P</i>
Hippocampus	-0.55	0.04*	0.05	0.82	-1.80	0.04
Exploratory regions	Pearson <i>r</i>	<i>P</i>	Pearson <i>r</i>	<i>P</i>	<i>z</i>	<i>P</i>
Entorhinal	-0.08	0.77	0.10	0.65	-0.49	0.31
Parahippocampal	-0.29	0.31	0.01	0.97	-0.83	0.20
Amygdala	-0.43	0.13	0.04	0.87	-1.34	0.09
Lateral temporal	-0.26	0.38	-0.10	0.65	-0.45	0.33
Prefrontal	-0.02	0.95	-0.21	0.32	0.52	0.30
PCC/precuneus	-0.12	0.69	-0.32	0.12	0.57	0.29
Anterior cingulate	0.07	0.80	-0.05	0.82	0.32	0.37
Lateral parietal	-0.18	0.53	-0.43	0.03*	0.75	0.23
Lateral occipital	-0.13	0.66	-0.32	0.13	0.54	0.30
Medial occipital	-0.10	0.73	-0.19	0.37	0.25	0.40
Pericentral	0.00	0.99	-0.17	0.44	0.46	0.32

Data are Pearson *r* and associated two-tailed *P* values obtained from separate univariate linear regression analyses in each group, uncorrected for multiple comparisons. Global A $\beta$  deposition was calculated by averaging values of [<sup>11</sup>C] PiB *DVR* from the bilateral prefrontal, lateral temporal, posterior cingulate/precuneus, and lateral parietal ROIs, weighted by volume. Global A $\beta$  deposition was then correlated with [<sup>11</sup>C]UCB-J *DVR* from the 4 medial temporal structures and 8 neocortical ROIs. To determine significant differences between group correlation coefficients, Fisher z-transformations and associated one-tailed *P* values were reported. \* denotes significant correlation, with *P* < 0.05. *Abbreviations:* PCC posterior cingulate cortex, PiB Pittsburgh Compound B, SV2A synaptic vesicle glycoprotein 2A, *DVR* distribution volume ratio using a whole cerebellum reference region, *ROI* region of interest, *aMCI* amnesic mild cognitive impairment

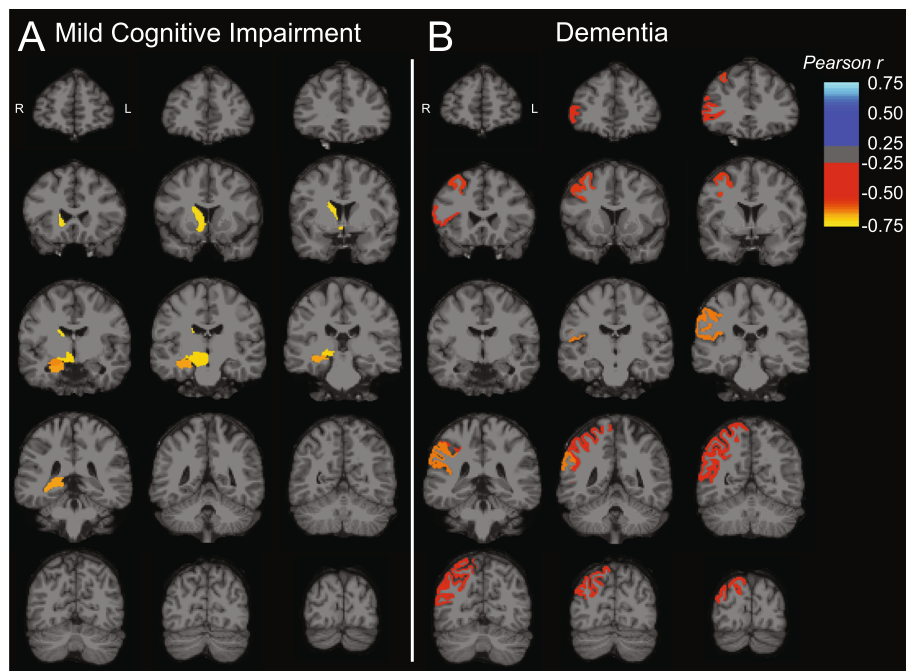


**Fig. 3** Brain maps of correlations between global A $\beta$  deposition and SV2A in aMCI and dementia. Brain maps were created by producing images with the voxels in each FreeSurfer region set uniformly to the calculated Pearson *r* for that region and overlaid on an MNI template T1 MRI. Correlations were across all 84 lateralized FreeSurfer brain regions and displayed only for regions with uncorrected *P* < 0.05 in both the **a** aMCI and **b** dementia diagnostic groups. MR image slices adhere to radiological convention, with orientation denoted in the first coronal section of each image series. *Abbreviations:* *DVR*, distribution volume ratio using a whole cerebellum reference region; *aMCI*, amnesic mild cognitive impairment

associations with SV2A binding were more widespread across the right frontal, right parietotemporal, and right lateral occipital cortices (Supplementary Figure 3B). No differences remained significant after permutation-based correction for multiple comparisons.

Correction for partial volume effects revealed similar results to those observed in non-corrected data across all correlational analyses, including associations between global A $\beta$  deposition and hippocampal SV2A binding (Supplementary Figure 4), global A $\beta$  deposition and SV2A binding in neocortical ROIs (Supplementary Table 4), and global A $\beta$  deposition and regional SV2A binding in all FreeSurfer regions (Supplementary Figure 5).

#### Association of regional A $\beta$ deposition and regional synaptic density in aMCI and dementia

Additional exploratory analyses investigated regional A $\beta$  deposition and suggested no broad associations with regional SV2A binding in either diagnostic group (Table 3). However, in the dementia group, a nominal inverse association was observed between medial occipital A $\beta$  deposition and SV2A binding ( $r = -0.46$ ,  $P = 0.02$ ). In addition, a positive correlation was detected between hippocampal A $\beta$  deposition and synaptic density in the dementia group ( $r = 0.63$ ,  $P = 0.001$ ) and was also present if the aMCI and dementia groups were combined ( $r = 0.53$ ,  $P = 0.001$ ).

Analyses investigating the relationship between regional A $\beta$  deposition and synaptic density in all FreeSurfer regions suggested few correlations in aMCI participants (Fig. 4a), while analyses restricted to

participants with dementia revealed inverse associations across bilateral prefrontal, temporal, and parietal, and occipital (both medial and lateral) cortical regions (Fig. 4b). These inverse associations were strongest in right-hemisphere regions. In addition, consistent with the previous analysis, positive correlations were observed in the bilateral hippocampi of dementia participants.

Correction for partial volume effects yielded similar results to those observed in non-corrected data across all correlational analyses, including associations between regional A $\beta$  deposition and SV2A binding in neocortical ROIs (Supplementary Table 5) and regional A $\beta$  deposition and regional SV2A binding in all FreeSurfer regions (Supplementary Figure 6).

#### Discussion

In this study, we investigated the association of cerebral A $\beta$  deposition using [ $^{11}\text{C}$ ] PiB and regional synaptic density using [ $^{11}\text{C}$ ]UCB-J. Overall, our analyses were consistent with previous research showing that A $\beta$  plaque burden is not well-correlated with indices of clinical severity. However, consistent with our hypothesis, we observed that in participants with aMCI (a stage of continued A $\beta$  accumulation), global A $\beta$  deposition was more strongly inversely associated with synaptic density in the hippocampus compared to those with dementia (a stage of relative A $\beta$  plateau). This stronger association survived PVC (Supplementary Figure 4) and thus is not driven primarily by atrophy. Secondary exploratory analyses across multiple ROIs and whole brain analyses suggested no broad or consistent associations between

**Table 3** Correlation of regional A $\beta$  deposition and regional SV2A in aMCI and dementia due to AD

Primary region	Mild cognitive impairment ( $n = 14$ )		Dementia ( $n = 24$ )	
	Pearson $r$	$P$	Pearson $r$	$P$
Hippocampus	0.40	0.16	0.63	0.001*
Exploratory regions	Pearson $r$	$P$	Pearson $r$	$P$
Entorhinal	-0.01	0.96	0.29	0.17
Parahippocampal	-0.45	0.10	0.18	0.40
Amygdala	0.03	0.92	0.35	0.09
Lateral temporal	-0.24	0.40	-0.10	0.64
Prefrontal	-0.04	0.88	-0.28	0.19
PCC/precuneus	-0.06	0.83	-0.23	0.29
Anterior cingulate	0.14	0.63	0.02	0.93
Lateral parietal	-0.13	0.65	-0.26	0.22
Lateral occipital	-0.02	0.96	-0.32	0.12
Medial occipital	0.03	0.91	-0.46	0.02*
Pericentral	0.09	0.77	-0.12	0.58

Data are Pearson  $r$  and associated two-tailed  $P$  values obtained from separate univariate linear regression analyses in each group, uncorrected for multiple comparisons. Correlations between regional [ $^{11}\text{C}$ ] PiB and [ $^{11}\text{C}$ ]UCB-J DVR were assessed within 4 medial temporal structures and 8 neocortical ROIs. \* denotes  $P < 0.05$ . Abbreviations: PCC posterior cingulate cortex, PiB Pittsburgh Compound B, SV2A synaptic vesicle glycoprotein 2A, DVR distribution volume ratio using a whole cerebellum reference region, ROI region of interest, aMCI amnesic mild cognitive impairment



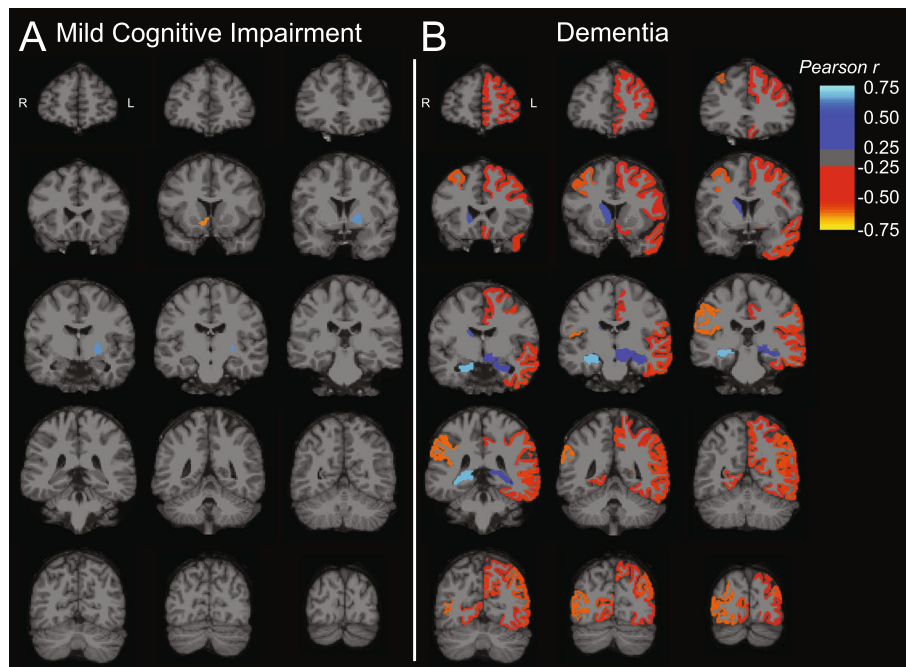


**Fig. 4** Brain maps of correlations between regional A $\beta$  deposition and SV2A in aMCI and dementia. Brain maps were created by producing images with the voxels in each FreeSurfer region set uniformly to the calculated Pearson  $r$  for that region and overlaid on an MNI template T1 MRI. Correlations were across all 84 lateralized FreeSurfer brain regions and displayed only for regions with uncorrected  $P < 0.05$  in both the **a** aMCI and **b** dementia diagnostic groups. MR image slices adhere to radiological convention, with orientation denoted in the first coronal section of each image series. Abbreviations: DVR, distribution volume ratio using a whole cerebellum reference region; aMCI, amnesic mild cognitive impairment

global A $\beta$  deposition and regional SV2A in either diagnostic group. The nominal negative associations with right-sided subcortical structures in aMCI but right-sided cortical regions with dementia participants (Fig. 3) in the full FreeSurfer region set are not fully mirrored in the corresponding surface-based analyses (Supplementary Figure 3) and may lack biological plausibility.

Additional exploratory ROI-based analyses of the association of regional A $\beta$  deposition and SV2A binding also revealed no consistent pattern but suggested a nominal inverse association in the dementia group between local A $\beta$  deposition and SV2A binding in medial occipital cortex. A more compelling, larger positive correlation was also observed between local A $\beta$  accumulation and synaptic density in the hippocampus (Table 3; Fig. 4). The latter “paradoxical” positive association (which is also present if the aMCI and dementia groups are combined) may relate to the fact that the hippocampus and other medial temporal lobe structures are atrophied to yield low signal with both PET tracers. However, the fact that this positive association is not impacted by PVC (including in the combined aMCI/dementia sample; Supplementary Table 5) suggests an alternative explanation. A theory that we have recently proposed [47–49] is that in early AD medial temporal lobe structures are degenerating so rapidly that the engine for A $\beta$  production is

severely compromised, resulting in low levels of A $\beta$  plaques in this region (Supplementary Table 2). In particular, the rapid early destruction of the entorhinal cortex may contribute to reduced A $\beta$  production by neurons that project to hippocampus. Thus, SV2A binding in the hippocampus may represent an index of viable perforant pathway neurons still capable of A $\beta$  production and release, and thus correlates with [ $^{11}\text{C}$ ] PiB binding in this region in AD.

#### Comparison to previous human studies of A $\beta$ deposition

Our overall results are consistent with prior evidence that A $\beta$  plaques are not well-correlated with indices of disease severity—at least in the dementia stage [27–29]—suggesting a dynamic balance between A $\beta$  deposition and clearance [28, 29]. They are also consistent with evidence from longitudinal PET studies that A $\beta$  deposition eventually approaches a plateau [30]. However, our finding that global A $\beta$  deposition was more strongly inversely associated with synaptic density in the hippocampus in participants with aMCI compared to those with dementia is also consistent with longitudinal PET studies. Such studies have demonstrated continued accumulation through the prodromal stages [31–33] but with minimal change by the time of conversion to AD dementia [31, 34] or in the dementia stage [35]. Our

results are further compatible with models of AD in which A $\beta$  initiates the cascade but later uncouples from neurodegenerative processes [34, 50, 51]. No previous study has examined the relationship between A $\beta$  plaque deposition and synaptic density in vivo. However, a number of studies have examined A $\beta$  deposition in relation to other measures of neurodegeneration, including MRI volumetry [52] and [ $^{18}\text{F}$ ]FDG-PET glucose metabolism [53], and have also observed this dissociation between A $\beta$  deposition and neurodegenerative changes.

#### Postmortem and in vitro studies of A $\beta$ and synapse density

Although no previous human studies have investigated in vivo the relationship between A $\beta$  accumulation and synaptic density, postmortem studies have provided limited evidence that soluble A $\beta$  species [7] and A $\beta$  oligomers (A $\beta$ o) [9] are associated with loss of synapses and synaptic proteins. However, measures of A $\beta$  deposition, A $\beta$ -immunoreactive plaques, thioflavin histofluorescent plaques, and concentrations of insoluble A $\beta$  have not been observed to correlate with synaptic change [7].

Non-human studies conducted in APP/PS1 transgenic mice have more fully explored the localized relationship between insoluble A $\beta$  and synapses, demonstrating a loss of synapses or dendritic spines in proximity to plaques [6, 10, 11]. These studies have also suggested a halo of neurotoxic soluble A $\beta$ o surrounding senile plaques, resulting in up to 60% loss of excitatory synapses within 50  $\mu\text{m}$  of the plaque [6]. Therefore, fibrillar A $\beta$  may act as a local reservoir of neurotoxic A $\beta$ o which results in the loss of proximal dendritic spines and synapses [6]. In the human brain, synaptic density has been observed to decrease progressively as the proximity to senile plaques increase, from normal levels of synaptic density at distances > 50  $\mu\text{m}$  away from the nearest plaque to a ~ 65% reduction in synaptic density levels near the edge of plaques (in association with A $\beta$ o concentrations) [8]. Our exploratory ROI-based analyses of the association of regional A $\beta$  deposition and SV2A binding revealed no consistent pattern and therefore cannot lend support to this model of fibrillar A $\beta$  (such as [ $^{11}\text{C}$ ] PiB is capable of measuring) acting as a local reservoir of synaptotoxic A $\beta$ o. However, our methods do not permit us to address highly localized (< 50  $\mu\text{m}$ ) associations.

#### Limitations

Important limitations of this study include the small sample size (aMCI = 14, dementia = 24) that hindered us from detecting regionally specific associations between A $\beta$  deposition and synaptic density across diagnostic groups. The other major limitation is the absence of longitudinal data that would enable us to study disease stage-specific relationships between A $\beta$  deposition and

synaptic density within participants. In particular, although we observed that in participants with aMCI, global A $\beta$  deposition was more strongly inversely associated with synaptic density in the hippocampus compared to those with dementia, we found no significant differences in mean A $\beta$  deposition ([ $^{11}\text{C}$ ] PiB DVR) between participants with aMCI and mild dementia (Supplementary Table 2). The latter finding may appear inconsistent with the notion that aMCI is a stage of continued A $\beta$  accumulation, while dementia is a stage of relative A $\beta$  plateau. This discrepancy may reflect the large inter-individual variability in A $\beta$  deposition that is present even at similar disease stages [30–34]. However, longitudinal studies would enable us to define stages of disease, including periods of A $\beta$  accumulation and plateau, within participants and to analyze the relationship between longitudinal changes in A $\beta$  deposition and synaptic loss.

#### Conclusions and future directions

To our knowledge, we have conducted the first in vivo study investigating the relationship between A $\beta$  deposition and synaptic alterations in participants with AD. We observed significant inverse associations between measures of global A $\beta$  deposition and hippocampal synaptic density within participants with aMCI but not with dementia. Our findings lend support to a model in which A $\beta$  is still accumulating in the early stages of clinical disease but approaching a relative plateau as a pool of primarily insoluble fibrillar A $\beta$ , a point at which A $\beta$  may uncouple from neurodegenerative processes including synaptic loss. Future research should investigate the relationship between A $\beta$  deposition and synaptic loss in larger cohorts (beginning at preclinical stages of AD) followed longitudinally in conjunction with other markers of pathogenesis.

#### Supplementary Information

The online version contains supplementary material available at <https://doi.org/10.1186/s13195-020-00742-y>.

##### Additional file 1: Supplementary Methods.

##### Additional file 2: Supplementary Figures and Tables.

Supplementary Figure 1. Correlation of DVR from 1TC modeling vs. SRTM2 with a cerebellar or CS reference region. Supplementary Table 1. Synaptic density in regions of interest. Supplementary Table 2. A $\beta$  deposition in regions of interest. Supplementary Table 3. Gray matter volume in regions of interest. Supplementary Figure 2. Comparison of SV2A and A $\beta$  deposition in CN, aMCI, and dementia groups after IY-PVC. Supplementary Figure 3. Surface-based, whole-cortex correlations between global A $\beta$  burden and SV2A in aMCI and dementia. Supplementary Figure 4. Correlation of global A $\beta$  deposition and hippocampal SV2A in aMCI and dementia after IY-PVC. Supplementary Table 4. Correlation of global A $\beta$  deposition and regional SV2A in aMCI and dementia after IY-PVC. Supplementary Figure 5. Brain maps of correlations between global A $\beta$  deposition and SV2A after IY-PVC. Supplementary Table 5. Correlation of regional A $\beta$  deposition and regional SV2A in aMCI and dementia after IY-PVC. Supplementary Figure 6. Brain maps of correlations between regional A $\beta$  deposition and SV2A after IY-PVC.

## Abbreviations

A $\beta$ : Amyloid- $\beta$ ; AD: Alzheimer's disease;  $BP_{ND}$ : Binding potential non-displaceable; Cb: Cerebellum; CDR: Clinical Dementia Rating Scale; CDR-SB: CDR sum of boxes; CN: Cognitively normal; CS: Centrum semiovale;  $DVR$ : Distribution volume ratio;  $DVR_{Cb}$ : Distribution volume ratio using a cerebellum reference region;  $DVR_{CS}$ : Distribution volume ratio using a centrum semiovale reference region; GDS: Geriatric depression scale; GM: Gray matter; IY: Iterative Yang; LMI: Logical Memory II; aMCI: Amnesic mild cognitive impairment; MMSE: Mini-Mental Status Exam; MRI: Magnetic resonance imaging; PCC: Posterior cingulate cortex; PET: Positron emission tomography; PVC: Partial volume correction; RAVLT: Rey Auditory Verbal Learning Test; SD: Standard deviation; ROI: Region of interest; SRTM2: Simplified reference tissue model—2 step; SV2A: Synaptic vesicle glycoprotein 2A; UPSIT: University of Pennsylvania Smell Identification Test;  $V_T$ : Volume of distribution (total); 1TC: 1 tissue compartment; PiB: Pittsburgh Compound B

## Acknowledgements

We wish to thank the research participants for their contributions, and the staff of the Yale ADRU and the Yale PET Center for their excellent technical assistance. We also thank UCB for providing the [ $^{11}C$ ]UCB-J radiolabeling precursor and the unlabeled reference standard.

## Authors' contributions

RSO, APM, REC, and ChvD contributed to the study concept and design. RSO, APM, MKC, MN, TT, YL, WZ, AFTA, REC, and ChvD contributed to the acquisition, analysis, or interpretation of the data. RSO, APM, and ChvD performed the statistical analysis. APM, REC, and ChvD obtained the funding. APM, MKC, TAG, JEH, HHB, ERB, VLK, NBN, JR, YY, BCWV, YH, REC, and ChvD provided administrative, technical, or material support. RSO, APM, and ChvD drafted the manuscript. All authors reviewed the manuscript, provided critical input, and approved the final manuscript.

## Funding

This research was supported by the National Institute on Aging (P50AG047270, K23AG057794, and R01AG052560, R01AG062276, RF1AG057553), the American Brain Foundation [APM], the Dana Foundation [MKC], the Thomas P. Detre Fellowship Award in Translational Neuroscience Research in Psychiatry [RSO], and the Ruth L. Kirschstein National Research Service Award, Clinical Neuroscience Research Training in Psychiatry (T32 2T32MH019961-21A1). This publication was made possible by CTSA Grant Number UL1 TR001863 from the National Center for Advancing Translational Science (NCATS), a component of the National Institutes of Health (NIH). The contents of this manuscript are solely the responsibility of the authors and the funding bodies had no role in the design of the study, data collection, analysis, interpretation, or writing of the manuscript.

## Availability of data and materials

The datasets used and/or analyzed in the current study are not publicly available but are available from the corresponding author on reasonable request. In addition, detailed methods and statistical analyses are made available in Additional file 1, while Supplementary Figures and Tables are made available in Additional file 2.

## Ethics approval and consent to participate

This study was approved by the Yale University Human Investigation Committee and the Yale Radioactive Drug Research Committee. In compliance with the Declaration of Helsinki, written informed consent was obtained from all participants and their study partners/caregivers prior to study participation.

## Consent for publication

All participants and study partners/caregivers gave written informed consent to participate in this investigational PET study for scientific purposes, including publications. The informed consents are available from the corresponding author upon reasonable request. All reported data are anonymized, and no individual participant information can be identified from the presented datasets.

## Competing interests

APM, REC, and ChvD report grants from National Institutes of Health for the conduct of the study. APM reports grants for clinical trials from Genentech and Eisai outside the submitted work. MKC reports research support from the Dana Foundation and research support from Eli Lilly and clinical trials from Merck outside the submitted work. YH reports research grants from the UCB and Eli Lilly outside the submitted work. YH, NBN, and REC have a patent for a newer version of the tracer. REC is a consultant for Rodin Therapeutics and has received research funding from UCB. REC reports having received grants from AstraZeneca, Astellas, Eli Lilly, Pfizer, Taisho, and UCB, outside the submitted work. ChvD reports consulting fees from Kyowa Kirin, Roche, Merck, Eli Lilly, and Janssen and grants for clinical trials from Biogen, Novartis, Eli Lilly, Merck, Eisai, Janssen, Roche, Genentech, Toyama, and Biohaven, outside the submitted work. No other disclosures are reported.

## Author details

<sup>1</sup>Alzheimer's Disease Research Unit, Yale University School of Medicine, One Church Street, 8th Floor, New Haven, CT 06510, USA. <sup>2</sup>Department of Psychiatry, Yale University School of Medicine, 300 George Street, New Haven, CT 06510, USA. <sup>3</sup>Department of Radiology and Biomedical Imaging, Yale University School of Medicine, P.O. Box 208048, New Haven, CT 06520, USA. <sup>4</sup>Program on Aging, Yale University School of Medicine, P.O. Box 207900, New Haven, CT 06520, USA. <sup>5</sup>Department of Neuroscience, Yale University School of Medicine, P.O. Box 208001, New Haven, CT 06520, USA. <sup>6</sup>Department of Neurology, Yale University School of Medicine, P.O. Box 208018, New Haven, CT 06520, USA.

Received: 8 September 2020 Accepted: 7 December 2020

Published online: 05 January 2021

## References

- Selkoe DJ. Alzheimer's disease is a synaptic failure. *Science*. 2002;298(5594):789–91.
- DeKosky ST, Scheff SW, Styren SD. Structural correlates of cognition in dementia: quantification and assessment of synapse change. *Neurodegeneration*. 1996;5(4):417–21.
- DeKosky ST, Scheff SW. Synapse loss in frontal cortex biopsies in Alzheimer's disease: correlation with cognitive severity. *Ann Neurol*. 1990;27(5):457–64.
- Shankar GM, Li S, Mehta TH, Garcia-Munoz A, Shepardson NE, Smith I, et al. Amyloid-beta protein dimers isolated directly from Alzheimer's brains impair synaptic plasticity and memory. *Nat Med*. 2008;14(8):837–42.
- Selkoe DJ, Hardy J. The amyloid hypothesis of Alzheimer's disease at 25 years. *EMBO Mol Med*. 2016;8(6):595–608.
- Koffie RM, Meyer-Luehmann M, Hashimoto T, Adams KW, Mielke ML, Garcia-Alloza M, et al. Oligomeric amyloid beta associates with postsynaptic densities and correlates with excitatory synapse loss near senile plaques. *Proc Natl Acad Sci U S A*. 2009;106(10):4012–7.
- Lue LF, Kuo YM, Roher AE, Brachova L, Shen Y, Sue L, et al. Soluble amyloid beta peptide concentration as a predictor of synaptic change in Alzheimer's disease. *Am J Pathol*. 1999;155(3):853–62.
- Koffie RM, Hashimoto T, Tai HC, Kay KR, Serrano-Pozo A, Joyner D, et al. Apolipoprotein E4 effects in Alzheimer's disease are mediated by synaptotoxic oligomeric amyloid-beta. *Brain*. 2012;135(Pt 7):2155–68.
- Pham E, Crews L, Ubhi K, Hansen L, Adame A, Cartier A, et al. Progressive accumulation of amyloid-beta oligomers in Alzheimer's disease and in amyloid precursor protein transgenic mice is accompanied by selective alterations in synaptic scaffold proteins. *FEBS J*. 2010;277(14):3051–67.
- Tsai J, Grutzendler J, Duff K, Gan WB. Fibrillar amyloid deposition leads to local synaptic abnormalities and breakage of neuronal branches. *Nat Neurosci*. 2004;7(11):1181–3.
- Spires TL, Meyer-Luehmann M, Stern EA, McLean PJ, Skoch J, Nguyen PT, et al. Dendritic spine abnormalities in amyloid precursor protein transgenic mice demonstrated by gene transfer and intravital multiphoton microscopy. *J Neurosci*. 2005;25(31):7278–87.
- Bajjalieh SM, Frantz GD, Weimann JM, McConnell SK, Scheller RH. Differential expression of synaptic vesicle protein 2 (SV2) isoforms. *J Neurosci*. 1994;14(9):5223–35.
- Bajjalieh SM, Peterson K, Linial M, Scheller RH. Brain contains two forms of synaptic vesicle protein 2. *Proc Natl Acad Sci U S A*. 1993;90(6):2150–4.

14. Nabulsi N, Mercier J, Holden D, Carre S, Najafzadeh S, Vandergeten MC, et al. Synthesis and preclinical evaluation of <sup>11</sup>C-UCB-J as a PET tracer for imaging the synaptic vesicle glycoprotein 2A in the brain. *J Nucl Med*. 2016; 57(5):777–84.
15. Finnema SJ, Nabulsi NB, Eid T, Detynecki K, Lin SF, Chen MK, et al. Imaging synaptic density in the living human brain. *Sci Transl Med*. 2016;8(348): 348ra96.
16. Finnema SJ, Nabulsi NB, Mercier J, Lin SF, Chen MK, Matuskey D, et al. Kinetic evaluation and test-retest reproducibility of [(11)C]UCB-J, a novel radioligand for positron emission tomography imaging of synaptic vesicle glycoprotein 2A in humans. *J Cereb Blood Flow Metab*. 2018;38(11):2041–52.
17. Chen MK, Mecca AP, Naganawa M, Finnema SJ, Toyonaga T, Lin SF, et al. Assessing synaptic density in Alzheimer disease with synaptic vesicle glycoprotein 2A positron emission tomographic imaging. *JAMA Neurol*. 2018;75(10):1215–24.
18. Mecca AP, Chen MK, O'Dell RS, Naganawa M, Toyonaga T, Godek TA, et al. In vivo measurement of widespread synaptic loss in Alzheimer's disease with SV2A PET. *Alzheimer's Dement*. 2020;16(7):974–82.
19. Masliah E, Mallory M, Hansen L, DeTeresa R, Alford M, Terry R. Synaptic and neuritic alterations during the progression of Alzheimer's disease. *Neurosci Lett*. 1994;174(1):67–72.
20. Scheff SW, Price DA, Schmitt FA, Mufson EJ. Hippocampal synaptic loss in early Alzheimer's disease and mild cognitive impairment. *Neurobiol Aging*. 2006;27(10):1372–84.
21. Scheff SW, Price DA, Schmitt FA, DeKosky ST, Mufson EJ. Synaptic alterations in CA1 in mild Alzheimer disease and mild cognitive impairment. *Neurology*. 2007;68(18):1501–8.
22. Scheff SW, Price DA, Schmitt FA, Scheff MA, Mufson EJ. Synaptic loss in the inferior temporal gyrus in mild cognitive impairment and Alzheimer's disease. *J Alzheimers Dis*. 2011;24(3):547–57.
23. Scheff SW, Price DA, Schmitt FA, Roberts KN, Ikonomic MD, Mufson EJ. Synapse stability in the precuneus early in the progression of Alzheimer's disease. *J Alzheimers Dis*. 2013;35(3):599–609.
24. Scheff SW, Price DA, Ansari MA, Roberts KN, Schmitt FA, Ikonomic MD, et al. Synaptic change in the posterior cingulate gyrus in the progression of Alzheimer's disease. *J Alzheimers Dis*. 2015;43(3):1073–90.
25. Braak H, Thal DR, Ghebremedhin E, Del Tredici K. Stages of the pathologic process in Alzheimer disease: age categories from 1 to 100 years. *J Neuropathol Exp Neurol*. 2011;70(11):960–9.
26. Gomez-Isla T, Price JL, McKeel DW Jr, Morris JC, Growdon JH, Hyman BT. Profound loss of layer II entorhinal cortex neurons occurs in very mild Alzheimer's disease. *J Neurosci*. 1996;16(14):4491–500.
27. Arriagada PV, Growdon JH, Hedley-Whyte ET, Hyman BT. Neurofibrillary tangles but not senile plaques parallel duration and severity of Alzheimer's disease. *Neurology*. 1992;42(3 Pt 1):631–9.
28. Hyman BT, Marzloff K, Arriagada PV. The lack of accumulation of senile plaques or amyloid burden in Alzheimer's disease suggests a dynamic balance between amyloid deposition and resolution. *J Neuropathol Exp Neurol*. 1993;52(6):594–600.
29. Ingelsson M, Fukumoto H, Newell KL, Growdon JH, Hedley-Whyte ET, Frosch MP, et al. Early Abeta accumulation and progressive synaptic loss, gliosis, and tangle formation in AD brain. *Neurology*. 2004;62(6):925–31.
30. Jack CR Jr, Wiste HJ, Lesnick TG, Weigand SD, Knopman DS, Vemuri P, et al. Brain beta-amyloid load approaches a plateau. *Neurology*. 2013;80(10):890–6.
31. Koivunen J, Scheinin N, Virta JR, Aalto S, Vahlberg T, Nagren K, et al. Amyloid PET imaging in patients with mild cognitive impairment: a 2-year follow-up study. *Neurology*. 2011;76(12):1085–90.
32. Villemagne VL, Pike KE, Chetelat G, Ellis KA, Mulligan RS, Bourgeat P, et al. Longitudinal assessment of Abeta and cognition in aging and Alzheimer disease. *Ann Neurol*. 2011;69(1):181–92.
33. Jack CR Jr, Lowe VJ, Weigand SD, Wiste HJ, Senjem ML, Knopman DS, et al. Serial PIB and MRI in normal, mild cognitive impairment and Alzheimer's disease: implications for sequence of pathological events in Alzheimer's disease. *Brain*. 2009;132(Pt 5):1355–65.
34. Ossenkoppele R, van Berckel BN, Prins ND. Amyloid imaging in prodromal Alzheimer's disease. *Alzheimers Res Ther*. 2011;3(5):26.
35. Engler H, Forsberg A, Almkvist O, Blomquist G, Larsson E, Savitcheva I, et al. Two-year follow-up of amyloid deposition in patients with Alzheimer's disease. *Brain*. 2006;129(Pt 11):2856–66.
36. McKhann GM, Knopman DS, Chertkow H, Hyman BT, Jack CR Jr, Kawas CH, et al. The diagnosis of dementia due to Alzheimer's disease: recommendations from the National Institute on Aging-Alzheimer's Association workgroups on diagnostic guidelines for Alzheimer's disease. *Alzheimer's Dement*. 2011;7(3):263–9.
37. Albert MS, DeKosky ST, Dickson D, Dubois B, Feldman HH, Fox NC, et al. The diagnosis of mild cognitive impairment due to Alzheimer's disease: recommendations from the National Institute on Aging-Alzheimer's Association workgroups on diagnostic guidelines for Alzheimer's disease. *Alzheimer's Dement*. 2011;7(3):270–9.
38. Mecca AP, Barcelos NM, Wang S, Bruck A, Nabulsi N, Planeta-Wilson B, et al. Cortical beta-amyloid burden, gray matter, and memory in adults at varying APOE epsilon4 risk for Alzheimer's disease. *Neurobiol Aging*. 2018;61:207–14.
39. Erlandsson K, Buvat I, Pretorius PH, Thomas BA, Hutton BF. A review of partial volume correction techniques for emission tomography and their applications in neurology, cardiology and oncology. *Phys Med Biol*. 2012; 57(21):R119–59.
40. Shidahara M, Thomas BA, Okamura N, Ibaraki M, Matsubara K, Oyama S, et al. A comparison of five partial volume correction methods for tau and amyloid PET imaging with [<sup>18</sup>F]THK5351 and [<sup>11</sup>C]PIB. *Ann Nucl Med*. 2017; 31(7):563–9.
41. de Jong HW, van Velden FH, Kloet RW, Buijs FL, Boellaard R, Lammertsma AA. Performance evaluation of the ECAT HRRT: an LSO-LYSO double layer high resolution, high sensitivity scanner. *Phys Med Biol*. 2007;52(5):1505–26.
42. Carson R, Barker W, Liow J, Adler S, Johnson C. Design of a motion-compensation OSEM list-mode algorithm for resolution-recovery reconstruction of the HRRT. Portland: IEEE Nuclear Sciences Symposium; 2003.
43. Jin X, Mulnix T, Gallezot JD, Carson RE. Evaluation of motion correction methods in human brain PET imaging—a simulation study based on human motion data. *Med Phys*. 2013;40(10):102503.
44. Fischl B. *FreeSurfer Neuroimage*. 2012;62(2):774–81.
45. Wu Y, Carson RE. Noise reduction in the simplified reference tissue model for neuroreceptor functional imaging. *J Cereb Blood Flow Metab*. 2002; 22(12):1440–52.
46. Rossano S, Toyonaga T, Finnema SJ, Naganawa M, Lu Y, Nabulsi N, et al. Assessment of a white matter reference region for (11) C-UCB-J PET quantification. *J Cereb Blood Flow Metab*. 2020;40(9):1890–901.
47. Paspalas CD, Carlyle BC, Leslie S, Preuss TM, Crimins JL, Huttner AJ, et al. The aged rhesus macaque manifests Braak stage III/IV Alzheimer's-like pathology. *Alzheimer's Dement*. 2018;14(5):680–91.
48. Arnsten AFT, Datta D, Leslie S, Yang ST, Wang M, Nairn AC. Alzheimer's-like pathology in aging rhesus macaques: unique opportunity to study the etiology and treatment of Alzheimer's disease. *Proc Natl Acad Sci U S A*. 2019;116(52):26230–38.
49. Arnsten AFT, Datta D, Tredici KD, Braak H. Hypothesis: tau pathology is an initiating factor in sporadic Alzheimer's disease. *Alzheimer's Dement*. 2020. <https://doi.org/10.1002/alz.12192>.
50. Hanseeuw BJ, Betensky RA, Jacobs HIL, Schultz AP, Sepulcre J, Becker JA, et al. Association of amyloid and tau with cognition in preclinical Alzheimer disease: a longitudinal study. *JAMA Neurol*. 2019;76(8):915–24.
51. Sperling RA, Mormino EC, Schultz AP, Betensky RA, Papp KV, Amariglio RE, et al. The impact of amyloid-beta and tau on prospective cognitive decline in older individuals. *Ann Neurol*. 2019;85(2):181–93.
52. Tosun D, Schuff N, Mathis CA, Jagust W, Weiner MW, Alzheimer's Disease Neuroimaging I. Spatial patterns of brain amyloid-beta burden and atrophy rate associations in mild cognitive impairment. *Brain*. 2011;134(Pt 4):1077–88.
53. Forster S, Grimmer T, Miederer I, Henriksen G, Yousefi BH, Graner P, et al. Regional expansion of hypometabolism in Alzheimer's disease follows amyloid deposition with temporal delay. *Biol Psychiatry*. 2012;71(9):792–7.

## Publisher's Note

Springer Nature remains neutral with regard to jurisdictional claims in published maps and institutional affiliations.